remote sensing

MDPI

Article

Quantifying Understory Complexity in Unmanaged Forests Using TLS and Identifying Some of Its Major Drivers

Dominik Seidel [1,*], Peter Annighöfer [2], Christian Ammer [1], Martin Ehbrecht [1], Katharina Willim [1], Jan Bannister [3] and Daniel P. Soto [4]

[1] Silviculture and Forest Ecology of the Temperate Zones, Faculty of Forest Sciences, University of Göttingen, Büsgenweg 1, 37077 Göttingen, Germany; Christian.Ammer@forst.uni-goettingen.de (C.A.); martin.ehbrecht@forst.uni-goettingen.de (M.E.); kwillim1@forst.uni-goettingen.de (K.W.)
[2] Forest and Agroforest Systems, Technical University of Munich, Hans-Carl-v.-Carlowitz-Platz 2, 85354 Freising, Germany; peter.annighoefer@tum.de
[3] Instituto Forestal, INFOR, Oficina Chiloé, Castro 7770223, Chile; jbannister@infor.cl
[4] Departamento de Ciencias Naturales y Tecnología, Universidad de Aysén, Coyhaique 5950000, Chile; daniel.soto@uaysen.cl
* Correspondence: dseidel@gwdg.de

Abstract: The structural complexity of the understory layer of forests or shrub layer vegetation in open shrublands affects many ecosystem functions and services provided by these ecosystems. We investigated how the basal area of the overstory layer, annual and seasonal precipitation, annual mean temperature, as well as light availability affect the structural complexity of the understory layer along a gradient from closed forests to open shrubland with only scattered trees. Using terrestrial laser scanning data and the understory complexity index (UCI), we measured the structural complexity of sites across a wide range of precipitation and temperature, also covering a gradient in light availability and basal area. We found significant relationships between the UCI and tree basal area as well as canopy openness. Structural equation models (SEMs) confirmed significant direct effects of seasonal precipitation on the UCI without mediation through basal area or canopy openness. However, annual precipitation and temperature effects on the UCI are mediated through canopy openness and basal area, respectively. Understory complexity is, despite clear dependencies on the available light and overall stand density, significantly and directly driven by climatic parameters, particularly the amount of precipitation during the driest month.

Keywords: forest structure; WorldClim2; precipitation gradient; old-growth; terrestrial laser scanning

Citation: Seidel, D.; Annighöfer, P.; Ammer, C.; Ehbrecht, M.; Willim, K.; Bannister, J.; Soto, D.P. Quantifying Understory Complexity in Unmanaged Forests Using TLS and Identifying Some of Its Major Drivers. *Remote Sens.* **2021**, *13*, 1513. https://doi.org/10.3390/rs13081513

Academic Editors: Markus Eichhorn and Ting Yun

Received: 4 March 2021
Accepted: 12 April 2021
Published: 14 April 2021

1. Introduction

The understory of a forest, as well as vegetation in shrublands without a distinct overstory, are important contributors to several ecosystem functions and services, including flora and fauna diversity [1–3]. Shrubby vegetation also affects nutrient cycling [4] and provides breeding and feeding grounds for large mammals [5]. In addition to these ecological functions, the understory layer determines the future species composition and structure of forests [6,7], which is of economic and ecological importance [8]. This is simply because juvenile trees—the so-called regeneration—are also part of the understory layer. In forests, the understory layer hence contains those trees that are potential future overstory trees through successional dynamics [9,10]. In shrublands with only scattered large trees, shrubby vegetation constitutes an important transitional habitat that results in high taxonomic and functional diversity [11].

Research on the development, composition, and structure of the understory layer in forests was largely motivated by the question of what conditions enabled the successful establishment of regeneration trees [10,12,13]. Forest managers require this knowledge to establish the regeneration of the forests with the desired tree species in order to control

timber production [14,15]. Particularly, the amount of light passing through the crowns of overstory trees was intensively studied as a key driver of regeneration and understory layer development [16–18]. However, other drivers of understory layer development have also been investigated, such as soil nitrogen and nutrient availability [17,19], competition for growing space [20], soil water content [21], and effects of fertilization [22], to name a few examples.

In the context of climate change, climatic effects on the understory layer development are of particular interest. In that way, substantial changes in structure and function for terrestrial ecosystems are expected [23]. Several studies have showed that understory layer development is sensitive to climatic drivers [24–26] but most studies were focused on abundance (counts or coverage) or diversity (diversity indices or species richness) of plants in the understory layer rather than understory layer "complexity". With regard to vegetation structures, this "complexity" is a summarizing term describing all dimensional, architectural and distributional patterns of plant individuals and their organs [27]. While the detailed structural complexity of the understory layer could not be measured objectively and quantitatively in the past, it is certainly an interesting characteristic since the structure and function of vegetation are closely related [28–31].

Recent advancements in methods for capturing the three-dimensional (3D) vegetation structure through terrestrial laser scanning (TLS) provide access to detailed information on the structure of forests [5,32–35]. In some of these approaches, vegetation complexity was assessed solely mathematically based on the three-dimensional distribution pattern of laser hits detected by laser scanners after active emission from the device (emission- reflection—capturing). Since the contribution of individual objects to the final complexity of a scene is not derived in such an approach, the derived complexity measures were named "holistic" measures [34–36]. One example, the stand structural complexity index (SSCI), was shown to be related to a number of conventional structural measures, such as Füldner's index of tree size differentiation, the Clark Evans Index of aggregation, the structural complexity index by Zenner and Hibbs, the Gini coefficient of diameters, as well as species diversity [34,37] and the abundance of microhabitats in a stand [38]. Another holistic measure of complexity, the box-dimension, was shown to be related to the degree of crown overlapping in a stand, as well as to the number of trees present, the overall space occupation and finally also to central tendencies of several architectural characteristics of the trees in a stand [36,39]. Furthermore, holistic measures such as the SSCI aligned with expert ratings of structural complexity [40]. These new tools allow one to directly investigate the drivers of vegetation complexity, rather than using surrogates to estimate it. In a recent study, [41] could show that precipitation is a key driver of stand structural complexity in unmanaged forests around the world, explaining as much as 89% of the variation in structural complexity.

The so-called understory complexity index (UCI) was recently introduced by [42] to describe the structural complexity of the understory layer as a whole, including the stems of overstory trees, shrubs, regeneration trees, and any other plant material located within 0.8 and 1.8 m above the forest floor. The index is based on a highly efficient single-scan approach, with each scan being independently analyzed to obtain information on the scanned scene, rather than several scans being co-registered during post-processing and merged into a single 3D dataset of the scene consisting of information from several viewpoints. The UCI makes use of the information on the spatial distribution of reflected laser beams in the previously mentioned height layer (0.8 and 1.8 m above the forest floor). Such a single-scan design (single perspective) certainly has limitations, most clearly the limited vertical extent of the layer that can be considered for analysis (here 1 m). The understory layer may extend well above or below this height layer. However, it is advantageous that the approach reduces field work (~3 min per sample point) drastically and, more importantly that it is entirely based on objective and quantitative measurements. An algorithm calculates the structural complexity of a scene (or selected area in a scene) purely based on the xyz-locations of vegetation hit by the laser beam and received back at the sensor after reflection. There is no subjectivity in the process. Previous studies showed

that the UCI was responsive to the presence of established regeneration trees (the more trees the higher the UCI) and the existence of skid-trails in European beech forests, with skid trails reducing the understory complexity significantly [42].

Here, we aimed at using this new index to investigate the structural complexity of vegetation between 0.8 and 1.8 m above ground across a climatic gradient in old-growth forests and a shrubland in Chile. It is worth mentioning that it was not our intention to depict the different elements that create complexity in this vegetation layer (herbs, shrubs, regeneration trees, overstory stems) but to quantify the general level of structural complexity in an objective and holistic way, and to investigate how it relates to the presence of overstory trees, to the available light, and to climatic parameters, namely precipitation and temperature.

We hypothesized that (i) the understory complexity index (UCI) is negatively related to the basal area at a site, as a higher basal area will result in greater competition for growing space and hence less favorable conditions for plant growth in the understory layer. We also hypothesized that (ii) an increase in canopy openness results in greater understory layer complexity due to increased light availability. Furthermore, we hypothesized (iii) that water availability is a key top–down driver of the complexity of the understory layer and hence UCI increases with mean annual precipitation and precipitation during the driest month. Finally, we hypothesized (iv) that the complexity of the understory layer increases with mean annual temperature.

2. Material and Methods

2.1. Study Sites

Between February and March 2019, we measured the complexity of vegetation between 0.8 and 1.8 m above ground across a gradient ranging from understory layers of temperate old-growth forests to the open conditions of a Mediterranean shrubland (see Figure 1). Our sites covered different overstory densities (basal area), light availabilities (canopy openness), a large gradient in precipitation and a notable range in mean annual temperature (Table 1). At five sites located in northern, central and southern Chile, we selected sampling areas that were undisturbed (unaffected by roads, hiking trails, nearby settlements) and without any signs of harvesting (e.g., stumps) to avoid anthropogenic influences (see Figure 1). Despite the effort, in the case of one site (Parque Nacional la Campana; from here on: La Campana), we observed some signs of livestock (cow dung) in some of the investigated patches. The soil moisture regime at two sites, La Campana and the Reserve las Chinchillas (from here on: Las Chinchillas), was xeric. All other sites were characterized by an udic soil moisture regime [43].

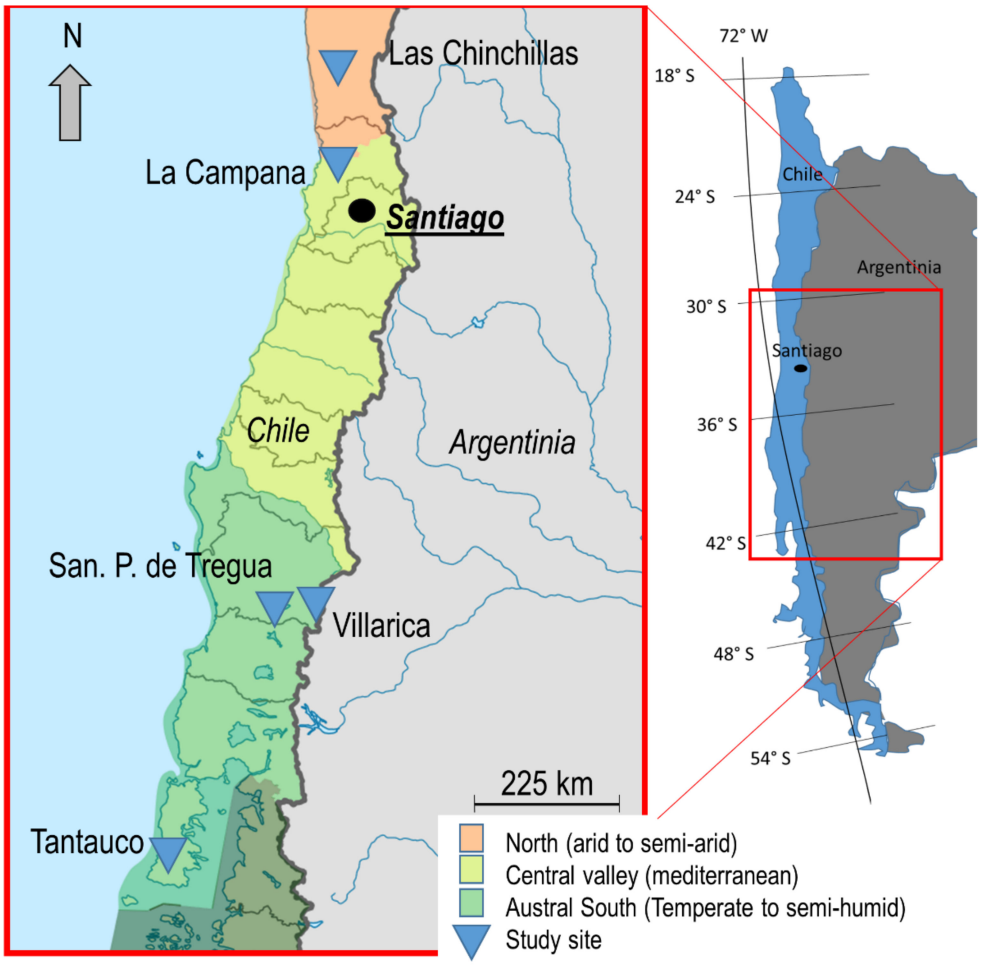

Figure 1. Map of the five study site locations in Chile.

2.2. Sampling Scheme and Scan Settings

At each site, we placed between three and nine sample plots, each consisting of five measurement positions for scanning with a spatial arrangement resembling a five on a dice (quadratic layout with an additional central position, see Figure 2) as introduced in [40] for a similar task. Avoiding hiking trails, as well as topographical issues such as canyons, steep slopes, or rivers, we selected the location of the plots by beginning at a random starting point without such issues in the area of interest and defined it as the center of the first plot. Since some of the investigated sites were rather small with regard to the available undisturbed areas (without nearby hiking trails or adjacent managed forest areas), the next plots were then selected randomly by proceeding to walk in one direction. Thereby, the minimum distance between two plots' edges was 60 m to avoid larger overlap in the scanned scenes (only 15 m around each scan are used during analysis, but see chapter 2.3 for details). Plots were then randomly located in terms of azimuth directions (random rotation around center point of the five-on-a-dice scheme). This sampling scheme, with 123 sample points, resulted in 27 plots, with only very few plots consisting of less than five sample points (Table 1). This was due to general inaccessibility of the plots, e.g., sample point in a river gorge. At each sample point, we estimated the basal area (m^2/ha) using the angle count approach [44] facilitated through a Dendrometer II device [45]. Table 1 provides an overview on the main characteristics of the sites.

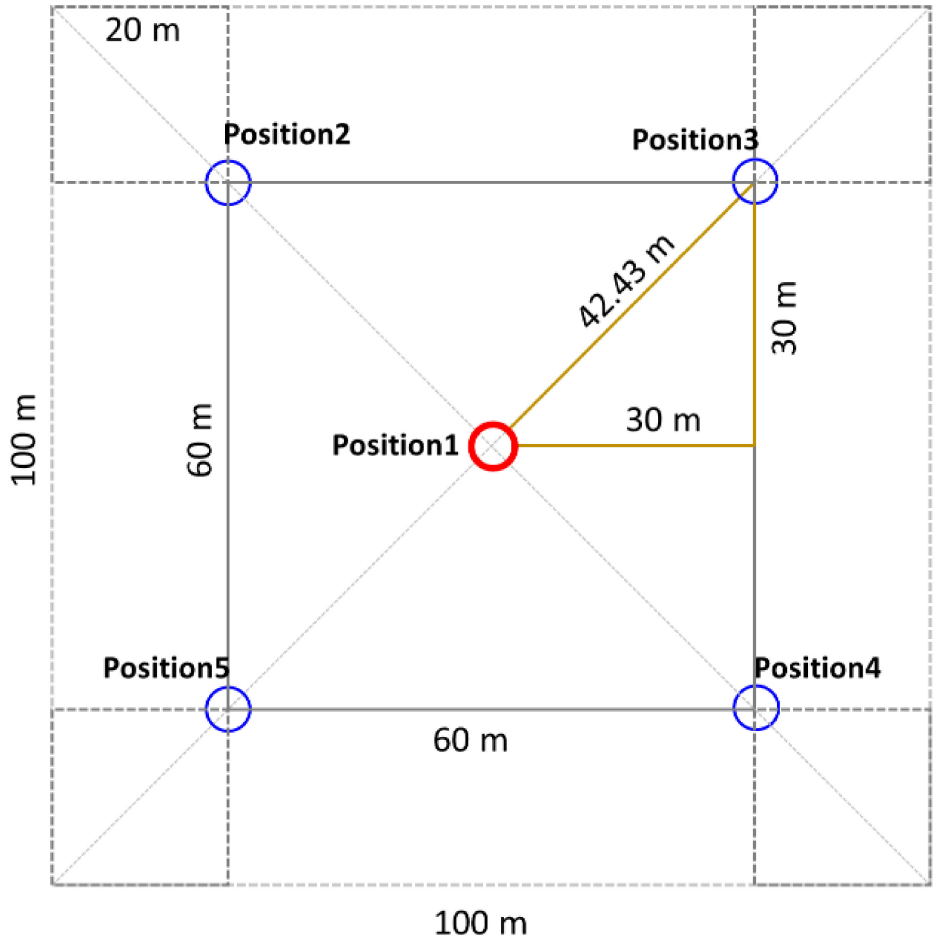

Figure 2. Sampling scheme at each plot with five scans per plot and a five-on-a-dice-like setup. The number of plots varied across sites, as depicted in Table 1, due to varying sizes of the investigated forest patches and accessibility.

On every sample point, we conducted a terrestrial laser scan using a Faro Focus M70 laser scanner (Faro Technologies, Lake Marry, USA) mounted and leveled on a standard tripod at breast height (1.3 m). The scanner was set to capture 300° and 360° in the vertical and horizontal direction, respectively. The angular step-width (scan resolution) was set to be 0.035 degrees and the maximum distance at which objects can be captured by the instrument was 70 m.

We conducted one scan at each sample point on every plot. A panoramic 2D-view on a typical scene for each site is shown in Figure 3.

Table 1. Main characteristics of the five investigated sites.

	Parque Tantauco	San Pablo de Tregua	Parque N. Villarica	Parque N. la Campana	Reserva Nacional las Chinchillas
Abbreviation	Tantauco	San P. de Tregua	Villarica	La Campana	Las Chinchillas
Geographical coordinates	43°1′4″ S 73°47′44″ W	39°36′14″ S 72°5′43″ W	39°34′54″ S 71°30′50″ W	32°56′41″ S 71°4′57″ W	31°30′28″ S 71°6′39″ W
Biogeographic region	South temperate [15]	North temperate [15]	North temperate [15]	South Mediterranean [15]	Central Mediterranean [15]
Bedrock	Metamorphic [1]	Volcanic ash [10]	Volcanic ash [11]	Granite [12]	Granite [13]
Soil moisture regime	Udic [14]	Udic [14]	Udic [14]	Xeric [14]	Xeric [14]
Landscape type	Forest	Forest	Forest	Forest	Shrubland
Region	Los Lagos	Los Rios	Araucania	Valparaiso	Coquimbo
Province	Chiloé	Valdivia	Cautín	Quillota	Chaopa
Nearest City	Quellón	Panguipulli	Curarrehue	Hijuelas	Illapel
Founded	2005	1972	1940	1967	1983
Management	Old-growth	Old-growth	Old-growth	Old-growth	Old-growth
Status	Private Park	Reserve	National Park	National Park	Reserve
Size (ha)	118.000	2.184	63.000	8.000	4.229
Mean annual temperature (°C) (1970–2000) [9]	9.39	8.35	6.78	14.42	14.09
Mean annual precipitation (mm) (1970–2000) [9]	2295.85	2055.43	1252.75	343.80	185.00
Main overstory tree species	ND, NB, DW, AL, SC, LP, PN [1,2,3]	ND, SC, LP [3,4,5]	AA, ND, NA, EC, ND [3,6]	JC, QS, LC, PCH, CA, AC, PB [3,7]	QS, LC, MB, PL, PCH [3,8]
Main understory tree species	Bt, Mc, DS, Cv, Lr [1,3]	Bt, Lr, Hi, Cv [3,5]	Pl, Lr, Lq [3]	Ech, Al, Bl, Co [3]	Ech, Al, Bl, Co [3]
No. of plots	9	7	3	4	4
No. of scans	33 *	35	15	20	20
Mean basal area (m^2/ha)	34.18	52.34	57.73	28.00	0.5
Mean canopy openness (%)	5	7	30	25	96

*** due to inaccessibility not all scan positions (sample points) per plot could be visited in Parque Tantauco. Sources:** [1] [46], [2] [47], [3] [48], [4] [49], [5] [50], [6] [51], [7] [52], [8] [53], [9] WorldClim Version 2 [54], [10] [55,56], [11] [56,57], [12] [57,58], [13] [53,56], [14] [43], [15] [59]. **Abbreviations (overstory species):** AC: *Acacia caven*; AL *Amomyrtus luma*; CA: *Cryptocaria alba*; DW: *Drimys winteri*; LC: *Lithraea caustica*; LP: *Laurelia philippiana*; MB: *Maytenus boaria*; NA: *Nothofagus alpina*; NB: *Nothofagus betuloides*; ND: *Nothofagus dombeyi*; NN: *Nothofagus nitida*; PB: *Peumus boldus*; PCH: *Prosopis chilensis*; PN: *Podocarpus nubigena*; QS: *Quillaja saponaria*; SC: *Saxegothaea conspicua*. **Abbreviations (understory species):** Al: *Azara lanceolate*; Bt: *Boquila trifoliolata*; Co: *Colliguaja odorifera*; Cv: *Campsidium valdivianum*; Ech: *Echinopsis chiloensis*; Hi: *Hygrangea intergerrima*; Lq: *Lophosoria quadripinnata*; Lr: *Luzuriaga radicans*; Pl: *Pseudopanax laetevirens*.

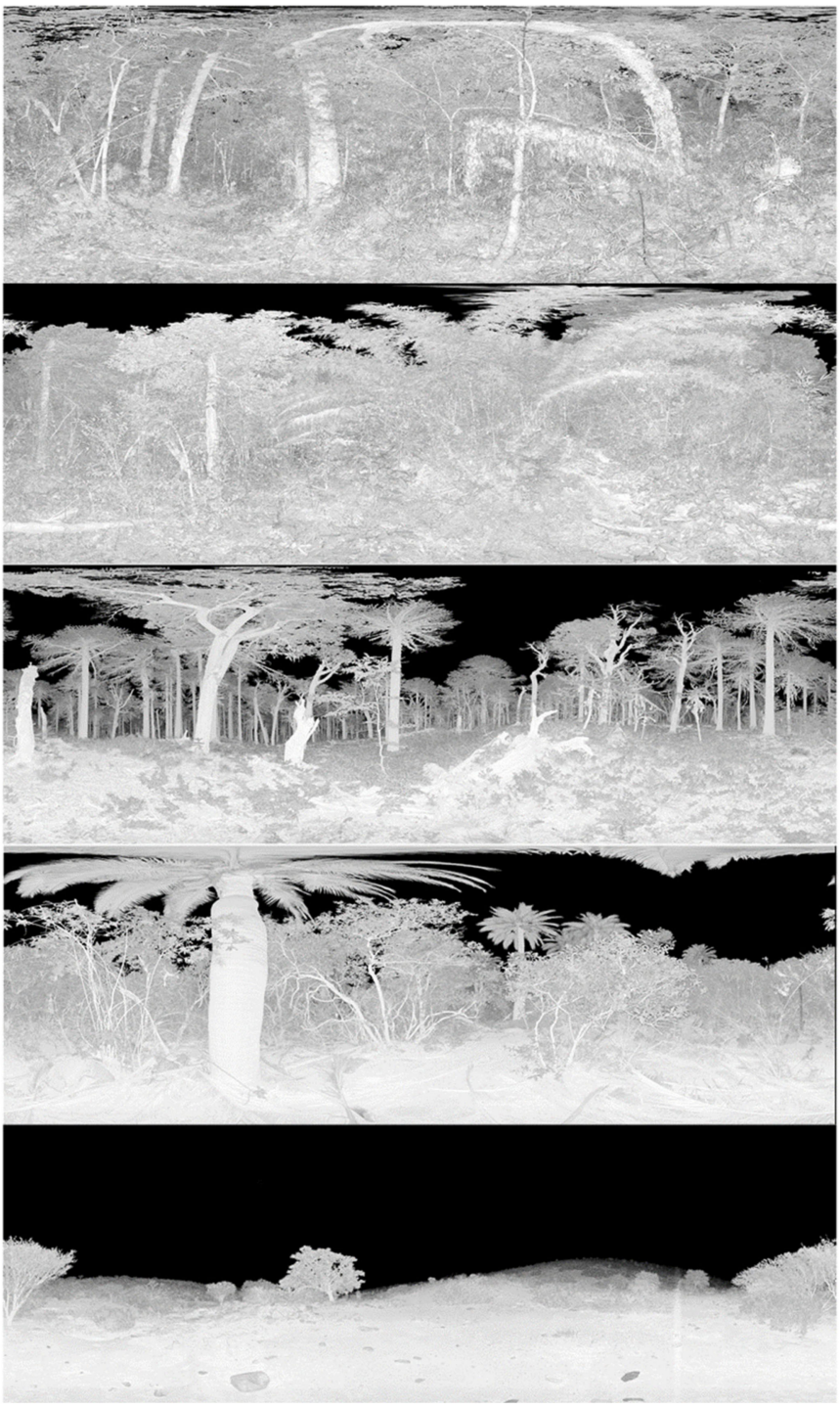

Figure 3. Exemplary 2D representation of the 3D data derived from the scans for each study site (panoramic views from single scans). From top to bottom: Tantauco, San P. d. Tregua, Villarica, La Campana and Las Chinchillas.

2.3. Calculation of Understory Layer Complexity and Canopy Openness from Laser Scans

All scans were individually treated as single scans in this study. First, using Faro Scene software (Faro Technologies, Lake Marry, Fl., USA), we filtered each scan for erroneous scan points applying the standard filters for isolated points, split laser beams, and low reflectivity. Then, each scan was exported as an xyz-file. Based on these files, we calculated the understory complexity index (UCI) as introduced by [42] using Mathematica software (Vers. 12, Wolfram Research, Champaign, IL, USA). To determine the UCI, first, the single

scan point clouds were limited to all data within 15 m horizontal distance to the scanner. Then, this circular patch of the xyz-data of the scanned scene was corrected for slope or undulation in the scanned area using normalized heights. These normalized heights are needed in order to address specific horizontal layers in a scene parallel to the ground. Normalized heights were based on a correction of each laser hits' vertical position (z-value of xyz-data) with the height of the underlying terrain derived from the scan through the interpolation of ground-hits [42]. From the normalized point cloud (ground-parallel data), a horizontal layer ranging from 0.8 to 1.8 m was extracted as presented in [42]. Due to the technical limitations of a single perspective of the scanner mounted on the tripod at 1.3 m height above ground, it is not recommended to consider a larger vertical layer. The layer or "slice" through the scenes, consisting of tree stems of adult trees, regeneration trees, shrubs and all other plant material reaching into this layer, was then considered the understory layer and characterized for its complexity. To do so, a polygon is created by connecting all hits based on their position (azimuth angle and distance to the scanner) after sorting them clockwise according to the azimuth angles. This polygon is more complex in shape when distances to hits of consecutive azimuth angles differ strongly when compared to distances that are fairly equal (cf. [42]). The degree of complexity of the shape of the polygon was finally determined using a modified version of the circumference-to-area ratio, the so-called fractal dimension index, introduced by [60], and originally designed for the analysis of the shape of landscape elements. The UCI cannot be strictly compared to conventional approaches that focus on specific objects, e.g., an inventory of regeneration trees or understory layer presence, a biomass assessment or an inventory of understory cover, as it does not distinguish different objects. It addresses the complexity of all vegetation present in this layer at once and summarizes it in a single number. Therefore, the UCI can be considered a holistic approach to complexity. For a more in-depth introduction of the UCI, the interested reader is referred to [42]. A graphical illustration of the procedure is depicted in Figure 4.

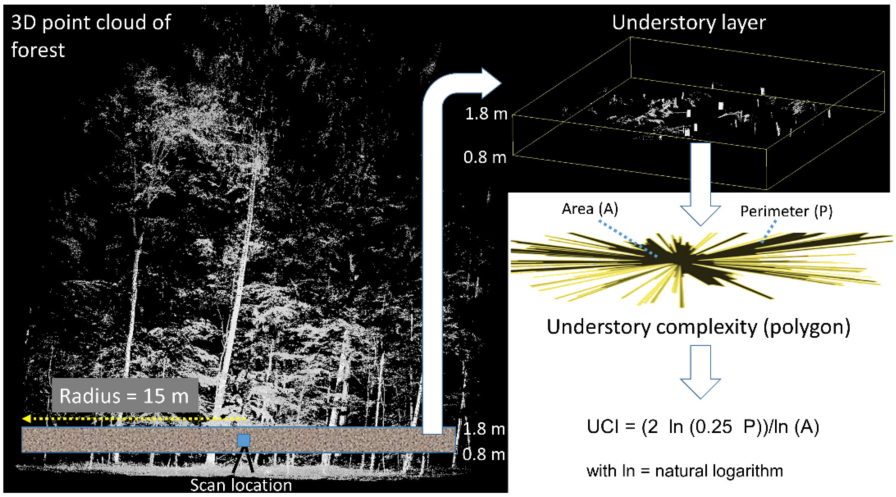

Figure 4. Graphical visualization of the calculation of the understory complexity index (UCI) based on a polygon connecting all hits in a horizontal layer of 1-m thickness centered at breast height (1.3 m).

In the following, canopy openness was derived from each scan following the approach presented in [61,62]. First, all points scanned at the respective scanning position were projected to the hemisphere described by the maximum scan distance (point distance was set to 70 m). Then, a stereographic projection was applied to create a circular image of the forest canopy similar to a hemispherical photograph. From this image, only the central area describing a 60° opening angle directly above the scanner was used for the calculation of canopy openness, defined as the area in the image uncovered by plant material and hence considered open sky (white pixels in the image) expressed as ratio (0 = no sky visible;

to 1 = no plant material visible (100% sky)). The reduced field of view (60° opening angle) is used to ensure that no areas are considered for the image that are out of reach of the scanner (range = 70 m). We conducted the procedure also in the shrubland site with only scattered trees, expecting canopy openness to reach as much as 100% in these cases.

2.4. Climate Data

We used the publicly available database WorldClim Version2 [54] to obtain the following climatic variables (averages for the years 1970–2000) from the 1 km-resolution dataset provided at the URL: https://www.worldclim.org/ (accessed on 20 August 2020). In this study, we used the mean annual precipitation, mean precipitation of the driest month and mean annual temperature to address precipitation effects, seasonality effects as well as effects of the temperature. All of these were shown to be of relevance for overall forest structural complexity in a recent study including some of our sites [41] and were therefore considered interesting climate attributes in our present study. Using the free software QGIS (Vers. 2.18 Las Palmas) and the "point sampling tool" plugin, we automatically collected the climate data for our sampling points based on the GPS location of every scan obtained during field work using a Garmin GPS-Map64 GPS device (Garmin AG, Schaffhausen, Switzerland).

2.5. Statistical Analysis

All data were aggregated to the plot level by taking the mean of all measures of all scans (usually five) per plot. This was carried out since reliable estimates of plot level understory structure should not be obtained from single-scan positions but from a sampling approach, as shown earlier [33,34,41]. The relationships among all explanatory variables for the UCI, namely the basal area, canopy openness and the climatic variables were first tested using Spearman's correlation analysis. Significant differences among means of the UCI across sites was tested using the ANOVA and Tukey post hoc test.

Relationships between the explanatory variables and the UCI were evaluated using non-linear generalized additive modeling (GAM) techniques [63]. This allowed one to not need to predefine the relationship between the response and explanatory variable, which results in an unbiased detection of the trends in the data themselves [64]. The effective degrees of freedom (EDF) were limited to a maximum of 3 (number of knots = 4), to avoid over-fitting of the data, with the amount of smoothing to be chosen automatically through generalized cross-validation [65]. EDF values around 1 point towards the linearity of the data; larger than 1 towards non-linear trends in the data. The data family was set to Gaussian type as the identity-link function [63]. In order to disentangle direct and mediated effects of climatic variables on the UCI, we used structural equation models (SEMs) as facilitated in the software Onyx [66]. We used a latent variable for the unknown error contribution to changes in the UCI and modelled the effect of mean annual precipitation, mean annual temperature, and precipitation in the driest month on the UCI. Thereby we modeled the direct effect of the variables on the UCI and the indirect effect through the basal area and canopy openness as mediators. We then evaluated the model performance (maximum likelihood models) based on the Akaike information criterion (AIC) and chi-quadrat statistics. The same was performed to investigate whether the interaction between the precipitation variables and mean annual temperature yield a significantly better prediction of the UCI than models considering only direct effects of the individual climatic variables. The significance level was $p < 0.05$ for all tests. All the statistical analyses were conducted using R (3.4.4, R Development Core Team). The used methods are visualized in the flow-chart shown in Figure 5.

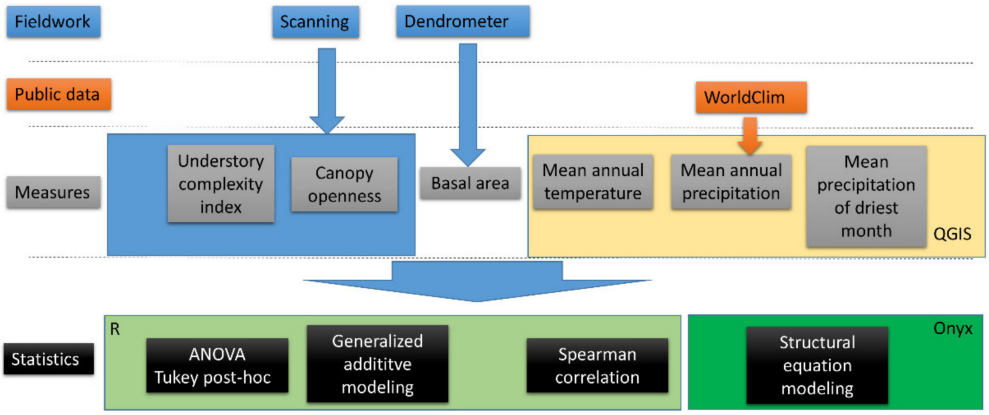

Figure 5. Methods flowchart of this study.

3. Results

We observed several relationships among the explanatory variables based on Spearman's correlation analysis (Table 2 and Figure 6).

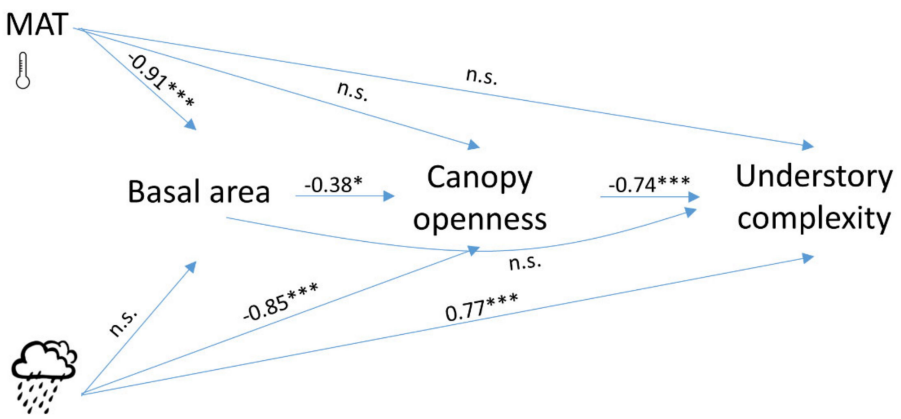

Figure 6. Graphical visualization of the relationships among all investigated explanatory variables and understory layer complexity accessed via Spearman's rho and the according significance of the relationship. *** = $p < 0.001$; * = $p < 0.05$; n.s. = not significant. MAT stands for mean annual temperature; cloud symbol indicates "mean annual precipitation".

Mean annual temperature had a significant negative effect on the basal area, while precipitation during the driest month or mean annual precipitation showed no correlation with the basal area. Both precipitation measures (annual and during driest month) affected the canopy openness negatively. The basal area and canopy openness were also significantly negatively correlated.

Overall, mean understory layer complexity (UCI) was highest in Tantauco, followed by San P. d. Tregua, Villarica and La Campana (no significant differences among these three) and lowest in the shrubland at Las Chinchillas with scattered trees only. Despite strong differences in the mean values, Tantauco and La Campana as well as Villarica and the Las Chinchillas were not significantly different from one another (Figure 7).

Table 2. Relationships among all explanatory variables accessed via Spearman's rho and the according *p*-values. A visualization of some of the relationships is also provided in Figure 6.

	Basal area	Canopy openness	Mean anual temperature	Mean anual precipitation	Mean precipitation of driest month
Basal area		−0.38	−0.91	0.32	0.34
Canopy openness	0.049		0.27	−0.85	−0.86
Mean anual temperature	<0.001	0.181		−0.27	−0.31
Mean anual precipitation	0.108	<0.001	0.174		0.98
Mean precipitation of driest month	0.084	<0.001	0.119	<0.001	

rho

p-values

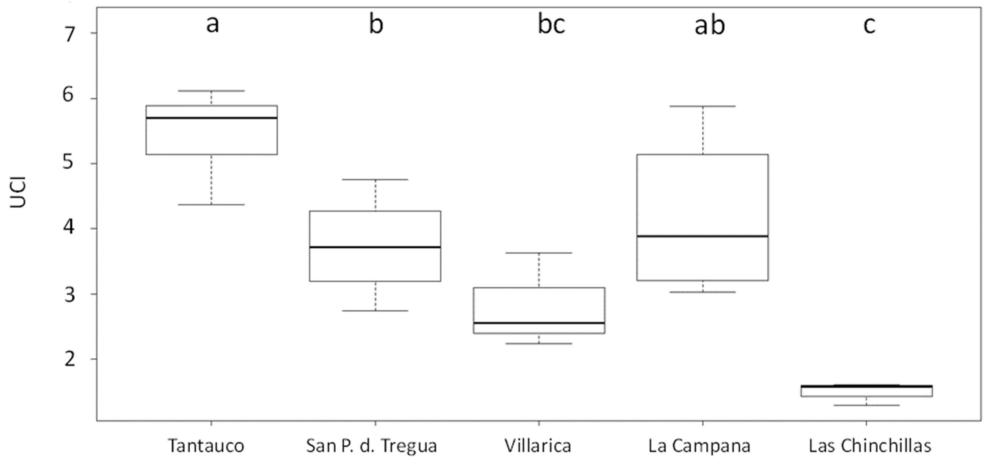

Figure 7. Box-and-whisker plot of the understory layer complexity, assessed using the understory complexity index (UCI) for each site. Different letters indicate significant differences among the means according to ANOVA and Tukey post hoc test. For the number of scans per site see Table 1.

The analysis based on generalized additive models revealed a significant hump-shaped relationship between the complexity of the understory layer, here described using the UCI, and the basal area present at a site (Figure 8).

With 66.5% explained deviance, the model showed a steep increase in the UCI from the shrubland site at Las Chinchillas, where only scattered trees were present (basal area between 1 and 2.5 m^2 ha^{-1}) towards the oasis-like forest of the La Campana with a basal area between 25 and 32 m^2 ha^{-1}. A further increase in basal area to 40 m^2 ha^{-1}, as observed in the dense forest of the Tantauco site, resulted in a maximized complexity of the understory layer. With further increase in basal area towards 70 m^2 ha^{-1}, the understory layer complexity decreased to 50% of the maximum and less.

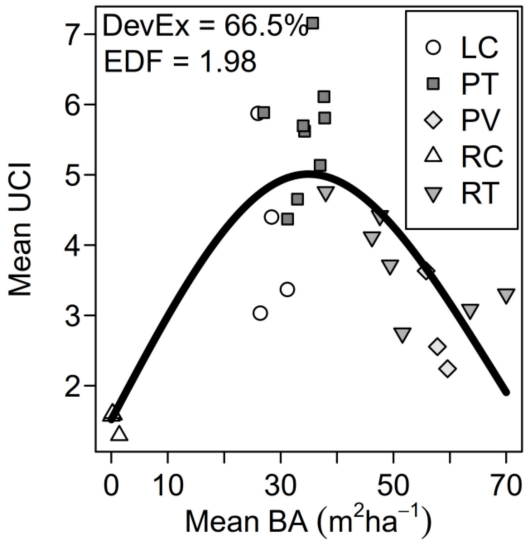

Figure 8. Relationship between the understory complexity index (UCI) as a measure of understory layer complexity and basal area (means per plot). DevEx = amount of deviance explained, EDF = effective degrees of freedom, LC = La Campana, PT = Parque Tantauco, PV = Parque Nacional Villarica, RC = Reserva Nacional las Chinchillas, RT = Reserva San Pablo de Tregua. Bold line: visualization of the fitted generalized additive modeling (GAM) model.

Furthermore, canopy openness affected the mean UCI significantly (deviation explained: 48.4%; see Figure 9). With increasing openness, the UCI successively dropped, reaching a minimum of just over one at 100% canopy openness. This relationship was, according to the GAM, not linear.

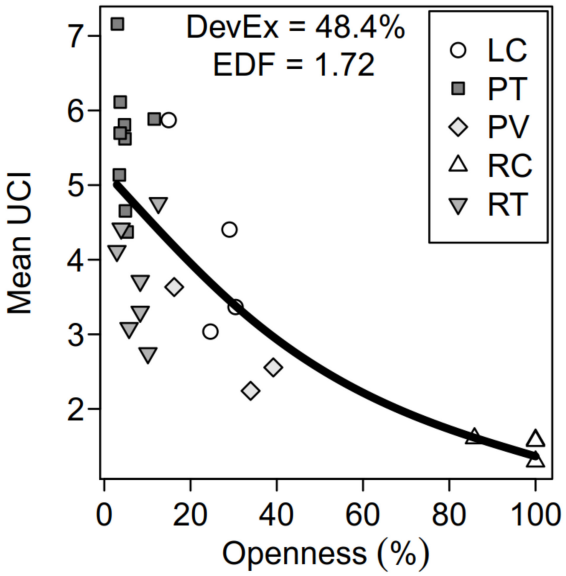

Figure 9. Relationship between mean canopy openness and mean understory layer complexity (UCI) for all sample plots. EDF = effective degrees of freedom. Bold line: visualization of the fitted GAM model.

We also found significant relationships between the tested climatic variables and the understory complexity index (Figure 10). A positive exponential relationship (deviation explained 48.4%) was detected between the mean annual precipitation and UCI (Figure 10A) and an even stronger (deviation explained 55.7%) but linear relationship between the mean precipitation of the driest month of the year and UCI (Figure 10B). For mean

annual temperature, we discovered a significant hump-shaped relationship with UCI (Figure 10C), however admitting a rather large gap in our data between 9.3° C and 14° C.

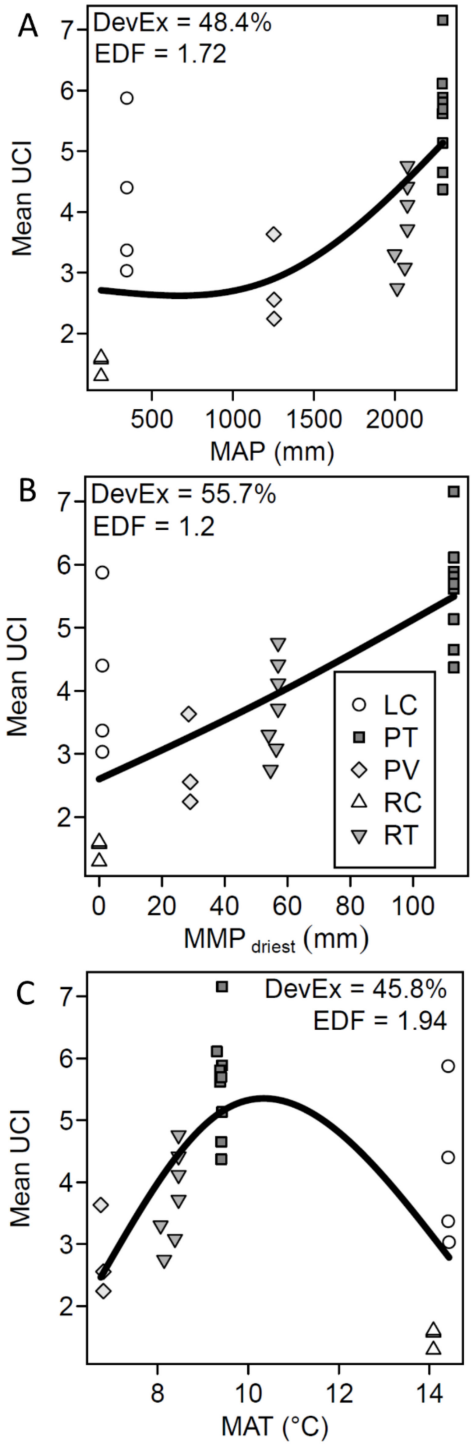

Figure 10. (**A**) Relationship between understory layer complexity assessed using the UCI and mean annual precipitation (MAP), (**B**) mean precipitation during the driest month of the year (MMP), and (**C**) mean annual temperature MAT). EDF = effective degrees of freedom. Bold lines: visualizations of the fitted GAM models. LC = Parque Nacional la Campana, PT = Parque Tantauco, PV = Parque Nacional Villarica, RC = Reserva Nacional las Chinchillas, RT = Reserva San Pablo de Tregua.

The analysis of direct vs. mediated effects through structural equation modelling revealed significant direct effects of precipitation on the UCI without mediation through the basal area, but only mediated effects of temperature on the UCI (mediated through the basal area). Furthermore, SEMs indicated a direct effect of precipitation during the driest month on the UCI without mediation of canopy openness, but not so for the annual precipitation. The UCI was not significantly better predicted using an SEM including the direct effects of mean annual precipitation when compared to one without the direct effect, modelling only the mediated effect through canopy openness. Finally, we found that the combined effect of the climatic variables yielded a significantly better prediction of UCI than models that considered only the direct effect of each variable individually and without interaction (see Table 3).

Table 3. Summary of the major properties of the compared structural equation models. Note: in every model we also used a latent variable for the error (soil differences, etc.) not shown in the first column. Brackets in the first column indicate that two variables were considered with their combined effect. The "►"-symbol indicates "effect of x on y". MAT = mean annual temperature; BA = basal area; UCI = understory complexity index; MMP = mean precipitation during driest month; CO = canopy openness; AIC = Akaike information criterion.

Structural Equation Models Compared	AIC	Chi-Square	*p*-Value
MMP ► BA ► UCI vs. MMP ► BA ► UCI + MMP ► UCI	235.9 vs. 217.7	20.2 vs. 0	<0.001
MAP ► BA ► UCI vs. MAP ► BA ► UCI + MAP ► UCI	227.1 vs. 214.5	14.6 vs. 0	<0.001
MAT ► BA ► UCI vs. MAT ► BA ► UCI + MAT ► UCI	208.5 vs. 209.8	0.7 vs. 0	Not significant
MAT ► CO ► UCI vs. MAT ► CO ► UCI + MAT ► UCI	203.5 vs. 201.0	4.5 vs. 0	<0.05
MAP ► CO ► UCI vs. MAP ► CO ► UCI + MAP ► UCI	129.5 vs. 191.2	0.2 vs. 0	Not significant
MMP ► CO ► UCI vs. MMP ► CO ► UCI + MMP ► UCI	199.7 vs. 195.0	6.7 vs. 0	<0.01
MAT ► UCI + MAP ► UCI vs. (MAP + MAT) ► UCI	217.1 vs. 193.8	27.3 vs. 0	<0.001
MAT ► UCI + MMP ► UCI vs. (MMP + MAT) ► UCI	215.9 vs. 208.7	11.1 vs. 0	<0.01

4. Discussion

In this study, we aimed for a better understanding of the drivers of understory layer complexity in the absence of management activities. In contrast to our hypothesis of a negative relationship between the basal area and the UCI (hypothesis (i)), we discovered a hump-shaped relationship. On the lower end of the gradient in the basal area, particularly

in the Mediterranean shrubland at Las Chinchillas, the UCI was extremely low despite the low basal area (Figure 8). We argue that the sites low in basal area were, despite the available growing space, too dry to enable the development of a complex shrub layer or an actual understory layer. This argument is supported by the results of the structural equation modelling, clearly indicating that precipitation had a significant direct effect on the UCI if modelled in addition to the mediated effect through the basal area (Table 3). Unfortunately, a gap exists in the basal area gradient in our data set, since we had no sites with basal areas between 3 and 26 m^2 ha^{-1}. This means our findings should be treated with caution, despite the GAMs and SEMs being significant. On the other end of the covered basal area gradient, on those sites with high basal area (Villarica and San P. d. Tregua), which are characterized by a few but tall trees forming a closed overstory layer, conditions were also not favorable for shrub layer complexity. Here, the negative effect of tall trees on the shrub layer development are clearly visible despite sufficient precipitation (Figure 8). Increased basal area resulted in reduced canopy openness (Table 2) which in turn resulted in reduced light availability on the forest floor (lower canopy openness) which consequently hampered understory layer development and complexity (cf. Figure 9). The results from [42], investigating humid beech forests in Europe, provide additional evidence for this argument, showing that the UCI was greatest when only very few overstory trees remained on the sites (low basal area, high canopy openness). This is also in line with earlier findings on the basal area–canopy openness relationship [67] or studies showing that even overstory tree height in a temperate forest is negatively related to understory layer density [68]. The negative effect of reduced light availability in the understory with high basal area on tree regeneration is well documented in the literature for various forest types [16,69–71]. However, at intermediate basal area (25-40 m^2/ha), our sites not only showed a large variation in understory layer complexity but also the highest values in general (optimum curve). A large variation in the UCI at a given basal area is not surprising and in fact should be expected. It has already been documented that there is a large heterogeneity in the understory of these old-growth forests [9,72]. The high understory layer complexity at the Tantauco site with intermediate basal areas can be explained through the favorable conditions for tree regeneration caused by natural tree death and single tree fall gaps, as well as beneficial climatic conditions in general (i.e., the moistest site). Additionally, in this forest, the regeneration of tree species is mostly from seeds and in elevated microsites over dead logs [73]. As mentioned earlier, the SEM approach also confirmed the strong direct effect of precipitation on the UCI even without mediation through the basal area (Table 3). Summarizing this, we can say that the basal area has a direct and negative effect on the UCI, even if precipitation is sufficient. Low basal areas, in contrast, do not have a direct causal contribution to the observed low UCIs, but rather did precipitation. This means that sites low in UCI are low in basal area because it is simply too dry for the development of a complex understory layer, or because overstory trees limit the resources available (high basal area) for understory layer development.

Surprisingly, and contrary to our expectation, we also have to reject hypothesis (ii) stating that an increase in canopy openness results in greater understory layer complexity. While there is a large literature presenting canopy openness (or other surrogates of light availability) as strong driver of understory layer growth and development [74–76] we found the opposite effect. We argue that in addition to different successional stages of dynamics not addressed here, the gradient of canopy openness covered in our data was determined by the large differences in climatic conditions at the sites rather than overstory disturbance per se. This is supported by the SEM approach, showing that models predicting the UCI from precipitation during the driest month or annual temperature performed significantly better if the direct effect of the climatic variables is included instead of using only the mediated effect through canopy openness (Table 3). Interestingly, this was not the case for mean annual precipitation. Here, we saw no significant improvement in model quality if the direct effect of mean annual precipitation on the UCI was explicitly modelled in addition to the mediated effect through canopy openness. This means, canopy openness

may be a crucial driver of UCI if climatic conditions are comparable, but it is rather a mediating agent for mean annual precipitation if looked at across biome borders, as carried out here (forest to shrubland transition). If precipitation is too low throughout the year, closed canopies are no longer possible and scattered trees will dominate (woodlands and shrublands). In our data, the driest site, Las Chinchillas, is also the most open site, with some plots having a canopy openness of as much as 100% (sky pixel fraction of 1) for the viewing angle considered here (60°). Hence, we have to reject our hypothesis (ii), as the positive effect of canopy openness on understory layer vegetation observed in many earlier studies [77] is in our case overruled by the climatic differences between the sites.

Considering the above, the plots at the La Campana had remarkably low openness values and high understory layer complexity given the low precipitation. For this site, we argue that a closed canopy is due to the presence of the characteristic Chilean Palm (*Jubaea Chilensis* (Molina) Baill.) on all plots scanned at La Campana, resulting in a higher than usual overstory density and lower canopy openness in the National Park (oasis character) when compared to the surrounding shrublands. In the shade of the palm trees, understory layer vegetation developed well despite low precipitation rates. In that way, spatial patterns show that trees of *J. chilensis* have a positive effect on the regeneration of other tree species, indicating a facilitation mechanism by producing semi-shade conditions, milding the air temperature and increasing the soil water availability [52]. This produces significant heterogeneity in the stands with clumped palm trees nested with understory trees, enhancing the understory layer complexity in this arid environment. This is supported by the large range of UCI at this site visible in Figure 7. However, our canopy openness data indicate that we missed a significant part of the gradient, not covering sites with an openness between 40% and 85%. Hence, caution is advised when trying to generalize these findings.

We confirmed our hypothesis (iii) by identifying relationships between the UCI and all tested climatic variables (Figure 10A–C). The positive effect of water availability (in general) on forest structure was reported earlier for forests in Patagonia [78–80]. The SSCI (stand structural complexity index), a holistic measure of structural complexity of the entire forest that is also based on single scans, was recently shown to be mostly driven by precipitation in primary forests around the world [41]. Other, more conventional measures related to forest structure, such as the normalized difference vegetation index (NDVI) were also shown to be related to the annual precipitation [81]. Overall, the relationship between precipitation and forest structure is of such strong manifestation that it is a key element in Holdridge's concept of life zones [82] and other global classifications of biomes [83]. We provide supporting evidence from our Chilean sites that a similar pattern exists for vegetation in the understory layer, with precipitation being clearly beneficial to the development of complex structures. For annual precipitation, the GAM approach even indicated that the relationship is exponential (Figure 10A). Furthermore, an even stronger (though linear) relationship between the UCI and precipitation during the driest month indicates that dry periods can be particularly threatening to the understory layer complexity (Figure 10B). Earlier studies already showed that seasonal precipitation is a stronger predictor of community productivity in forests than annual precipitation [84]. [41] provided strong evidence for precipitation seasonality also being crucial for stand structural complexity across biomes. We can extend this by stating that seasonal precipitation is also a strong predictor of understory layer complexity (Figure 10A vs. Figure 10B). Vegetation is known to be sensitive to the timing and magnitude of droughts and this was particularly shown for water-limited regions [85], also represented by our driest site with the lowest understory layer complexity (Las Chinchillas). Furthermore, we could show that the effect of precipitation on the UCI is a direct one (Table 3), and not only mediated through a lower basal area and hence reduced competition for water.

Finally, we could show that the temperature–understory layer complexity relationship in Chile does not follow a linear scheme, but is better described by an optimum-curve (rejection of hypothesis (iv)). Beyond a certain point (~11°C mean annual temperature),

temperature appeared to be not beneficial anymore to the development of a complex understory layer at the investigated sites. However, it is likely that the negative effect of temperature beyond an optimum was directly associated with the fact that the two warmest sites investigated were also the driest, with precipitation dropping to as little as 185 mm to 343 mm per year (cf. Table 1 for Las Chinchillas and La Campana). Therefore, it is rather the limited water supply than the temperature per se that limited the development of a complex understory layer. This is further supported by the better performance of models that predict the UCI from combined effects of temperature and precipitation (Table 3). In that regard, future studies in tropical sites may help to understand the understory layer complexity–temperature relationship for conditions with high temperatures in combination with sufficient precipitation.

5. Conclusions

We conclude that understory layer complexity, as determined by the understory complexity index, in unmanaged Chilean landscapes is strongly driven by climatic variables (temperature and precipitation). While there are known close relationships between stand density (basal area) as well as light availability (canopy openness) and understory layer development, we could show that there are also direct effects of the climate on the understory layer complexity. We observed a similar pattern for the understory layer as those depicted for entire forests in the concepts of global life zones or biomes. The concept of life zones of Holdridge [82], Whittaker [83], and others created theoretical models that related temperature, precipitation (and in the case of Holdridge also to evapotranspiration) to typical biomes or life zones characterized by typical vegetation types. These vegetation types were not described using species identities, but by using typical formations, e.g., "rainforest". We argue that these characterizations, though not based on quantitative data, were based on typical vegetation structures. The qualitative description of these structures, e.g., by [83], indicated a greater vegetation complexity in humid and warm climates. Only a few studies have attempted to provide empirical evidence for these patterns [41,86]. Here, we provide evidence from sites in Chile situated along a large climatic gradient. Understory layer complexity is strongly driven by precipitation and temperature, particularly by precipitation during the driest month. This holds implications for climate change scenarios, with extended droughts threatening the complexity of the understory layer and hence related ecosystem functions and services.

Author Contributions: D.S., D.P.S.; methodology: D.S., K.W.; software (Mathematica coding, Onyx, Faro Scene): D.S.; validation: D.S., P.A., J.B., D.P.S.; formal analysis: D.S., P.A.; investigation: D.P.S., D.S.; resources: D.S., D.P.S.; data curation: D.S., M.E., P.A.; writing—original draft: D.S.; writing—review and editing: D.S., P.A., C.A., M.E., K.W., J.B., D.P.S.; visualization: P.A., D.S.; supervision: D.S.; project administration: D.S., D.P.S.; funding acquisition: D.S., D.P.S. All authors have read and agreed to the published version of the manuscript.

Funding: This study was funded by DFG grant SE 2383/5-1 and Fondecyt 11181140.

Institutional Review Board Statement: Not applicable.

Informed Consent Statement: Not applicable.

Data Availability Statement: The data is available at https://data.goettingen-research-online.de/dataset.xhtml?persistentId=doi:10.25625/KAYFIQ (accessed on 20 August 2020).

Acknowledgments: The German Research Foundation (DFG) is acknowledged for funding this research through grant SE2383/5-1 provided to Dominik Seidel. Daniel Soto is thankful for the support of Fondecyt 11181140, and Fondo Semilla de Producción Científica -Universidad de Aysén. Jan Bannister thanks the support of MINAGRI.

Conflicts of Interest: The authors declare no conflict of interest.

References

1. Augusto, L.; Dupouey, J.-L.; Ranger, J. Effects of tree species on understory vegetation and environmental conditions in temperate forests. *Ann. For. Sci.* **2003**, *60*, 823–831. [CrossRef]
2. Hartley, M.J. Rationale and methods for conserving biodiversity in plantation forests. *For. Ecol. Manag.* **2002**, *155*, 81–95. [CrossRef]
3. Thomas, S.C.; Halpern, C.B.; Falk, D.A.; Liguori, D.A.; Austin, K.A. Plant diversity in managed forests: Understory responses to thinning and fertilization. *Ecol. Appl.* **1999**, *9*, 864–879. [CrossRef]
4. Kimmins, J.P. The Biogeochemical Cycle: Nutrient Cycling Within Ecosystems. In *Forest Ecology: A Foundation for Sustainable Forest Management and Environmental Ethics in Forestry*, 3rd ed.; Prentice Hall: Upper Saddle River, NJ, USA, 2004; pp. 103–104.
5. Eichhorn, M.P.; Ryding, J.; Smith, M.J.; Gill, R.M.; Siriwardena, G.M.; Fuller, R.J. Effects of deer on woodland structure revealed through terrestrial laser scanning. *J. Appl. Ecol.* **2017**, *54*, 1615–1626. [CrossRef]
6. Antos, J.A. Understory Plants in Temperate Forests. *For. For. Plants* **2009**, *1*, 262–279.
7. Soto, D.P.; Donoso, P.J. Patrones de regeneración en renovales de Drimys winteri en el centro-norte de la Isla de Chiloé: Cambios de acuerdo al tamaño y la densidad relativa. *Bosque* **2006**, *27*, 241–249.
8. Lu, H.C.; Buongiorno, J. Long-and short-term effects of alternative cutting regimes on economic returns and ecological diversity in mixed-species forests. *For. Ecol. Manag.* **1993**, *58*, 173–192. [CrossRef]
9. Donoso, P.J.; Nyland, R.D. Densidad de plántulas de acuerdo a la estructura, dominancia y cobertura del sotobosque en bosques siempreverdes adultos en la cordillera de la Costa de Chile. *Rev. Chil. Hist. Nat.* **2005**, *78*, 51–63.
10. Soto, D.P.; Puettmann, K.J.; Fuente, C.; Jacobs, D.F. Regeneration niches in Nothofagus-dominated old-growth forests after partial disturbance: Insights to overcome arrested succession. *For. Ecol. Manag.* **2019**, *445*, 26–36. [CrossRef]
11. Teste, F.P.; Kardol, P.; Turner, B.L.; Wardle, D.A.; Zemunik, G.; Renton, M.; Laliberté, E. Plant-soil feedback and the maintenance of diversity in Mediterranean-climate shrublands. *Science* **2017**, *355*, 173–176. [CrossRef] [PubMed]
12. Liira, J.; Sepp, T.; Kohv, K. The ecology of tree regeneration in mature and old forests: Combined knowledge for sustainable forest management. *J. For. Res.* **2011**, *16*, 184–193. [CrossRef]
13. Stiers, M.; Willim, K.; Seidel, D.; Ehbrecht, M.; Kabal, M.; Ammer, C.; Annighöfer, P. A quantitative comparison of the structural complexity of managed, lately unmanaged and primary European beech (*Fagus sylvatica* L.) forests. *For. Ecol. Manag.* **2018**, *430*, 357–365. [CrossRef]
14. Puettmann, K.J.; Ammer, C. Trends in North American and European regeneration research under the ecosystem management paradigm. *Eur. J. For. Res.* **2007**, *126*, 1–9. [CrossRef]
15. Soto, D.P.; Puettmann, K.J. Topsoil removal through scarification improves natural regeneration in high-graded Nothofagus old-growth forests. *J. Appl. Ecol.* **2018**, *55*, 967–976. [CrossRef]
16. Donoso, P.J.; Soto, D.P.; Coopman, R.E.; Rodríguez-Bertos, S. Early performance of planted Nothofagus dombeyi and Nothofagus alpina in response to light availability and gap size in a high-graded forest in the south-central Andes of Chile. *Bosque* **2013**, *34*, 23–32. [CrossRef]
17. Pacala, S.W.; Canham, C.D.; Saponara, J.; Silander, J.A., Jr.; Kobe, R.K.; Ribbens, E. Forest models defined by field measurements: Estimation, error analysis and dynamics. *Ecol. Monogr.* **1996**, *66*, 1–43. [CrossRef]
18. Soto, D.P.; Jacobs, D.F.; Salas, C.; Donoso, P.J.; Fuentes, C.; Puettmann, K.J. Light and nitrogen interact to influence regeneration in old-growth Nothofagus-dominated forests in south-central Chile. *For. Ecol. Manag.* **2017**, *384*, 303–313. [CrossRef]
19. Catovsky, S.; Kobe, R.K.; Bazzaz, F.A. Nitrogen-induced changes in seedling regeneration and dynamics of mixed coniferbroad-leaved forests. *Ecol. Appl.* **2002**, *12*, 1611–1625.
20. Annighöfer, P.J.; Seidel, D.; Mölder, A.; Ammer, C. Advanced aboveground spatial analysis as proxy for the competitive environment affecting sapling development. *Front. Plant Sci.* **2019**, *10*, 690. [CrossRef]
21. Madsen, P. Effects of soil water content, fertilization, light, weed competition and seedbed type on natural regeneration of beech (*Fagus sylvatica*). *For. Ecol. Manag.* **1995**, *72*, 251–264. [CrossRef]
22. Ceccon, E.; Huante, P.; Campo, J. Effects of nitrogen and phosphorus fertilization on the survival and recruitment of seedlings of dominant tree species in two abandoned tropical dry forests in Yucatán, Mexico. *For. Ecol. Manag.* **2003**, *182*, 387–402. [CrossRef]
23. Hannah, L.; Midgley, G.; Millar, D. Climate change-integrated conservation strategies. *Glob. Ecol. Biogeogr.* **2002**, *11*, 485–495. [CrossRef]
24. Couralet, C.; Sterck, F.J.; Sass-Klaassen, U.; Van Acker, J.; Beeckman, H. Species-specific growth responses to climate variations in understory trees of a Central African rain forest. *Biotropica* **2010**, *42*, 503–511. [CrossRef]
25. Hurteau, M.; North, M. Mixed-conifer understory response to climate change, nitrogen, and fire. *Glob. Chang. Biol.* **2008**, *14*, 1543–1552. [CrossRef]
26. Tsuyama, I.; Nakao, K.; Matsui, T.; Higa, M.; Horikawa, M.; Kominami, Y.; Tanaka, N. Climatic controls of a keystone understory species, Sasamorpha borealis, and an impact assessment of climate change in Japan. *Ann. For. Sci.* **2011**, *68*, 689–699. [CrossRef]
27. McElhinny, C.; Gibbons, P.; Brack, C.; Bauhus, J. Forest and woodland stand structural complexity: Its definition and measurement. *For. Ecol. Manag.* **2005**, *218*, 1–24. [CrossRef]
28. Davies, A.B.; Asner, G.P. Advances in animal ecology from 3D-LiDAR ecosystem mapping. *Trends Ecol. Evol.* **2014**, *29*, 681–691. [CrossRef] [PubMed]

29. Forrester, D.I.; Bauhus, J. A review of processes behind diversity—productivity relationships in forests. *Curr. For. Rep.* **2016**, *2*, 45–61. [CrossRef]
30. Gough, C.M.; Atkins, J.W.; Fahey, R.T.; Hardiman, B.S. High rates of primary production in structurally complex forests. *Ecology* **2019**, *100*, e02864. [CrossRef]
31. Luyssaert, S.; Schulze, E.D.; Börner, A.; Knohl, A.; Hessenmöller, D.; Law, B.E.; Ciais, P.; Grace, J. Old-growth forests as global carbon sinks. *Nature* **2008**, *455*, 213–215. [CrossRef] [PubMed]
32. Seidel, D.; Albert, K.; Fehrmann, L.; Ammer, C. The potential of terrestrial laser scanning for the estimation of understory biomass in coppice-with-standard systems. *Biomass Bioenergy* **2012**, *47*, 20–25. [CrossRef]
33. Seidel, D.; Ehbrecht, M.; Puettmann, K.J. Assessing different components of three-dimensional forest structure with single-scan terrestrial laser scanning: A case study. *For. Ecol. Manag.* **2016**, *381*, 196–208. [CrossRef]
34. Ehbrecht, M.; Schall, P.; Ammer, C.; Seidel, D. Quantifying stand structural complexity and its relationship with forest management, tree species diversity and microclimate. *Agric. For. Meteorol.* **2017**, *242*, 1–9. [CrossRef]
35. Seidel, D. A holistic approach to determine tree structural complexity based on laser scanning data and fractal analysis. *Ecol. Evol.* **2018**, *8*, 128–134. [CrossRef] [PubMed]
36. Seidel, D.; Ehbrecht, M.; Dorji, Y.; Jambay, J.; Ammer, C.; Annighöfer, P. Identifying architectural characteristics that determine tree structural complexity. *Trees* **2019**, *33*, 911–919. [CrossRef]
37. Juchheim, J.; Ehbrecht, M.; Schall, P.; Ammer, C.; Seidel, D. Effect of tree species mixing on stand structural complexity. *For. Int. J. For. Res.* **2020**, *93*, 75–83. [CrossRef]
38. Frey, J.; Asbeck, T.; Bauhus, J. Predicting tree-related microhabitats by multisensor close-range remote sensing structural parameters for the selection of retention elements. *Remote Sens.* **2020**, *12*, 867. [CrossRef]
39. Seidel, D.; Ehbrecht, M.; Annighöfer, P.; Ammer, C. From tree to stand-level structural complexity—Which properties make a forest stand complex? *Agricultural and Forest Meteorology* **2019**, *278*, 107699. [CrossRef]
40. Frey, J.; Joa, B.; Schraml, U.; Koch, B. Same viewpoint different perspectives—A comparison of expert ratings with a TLS derived forest stand structural complexity index. *Remote Sens.* **2019**, *11*, 1137. [CrossRef]
41. Ehbrecht, M.; Seidel, D.; Annighöfer, P.; Kreft, H.; Köhler, M.; Zemp, D.C.; Puettmann, K.; Nilus, R.; Babweteera, F.; Willim, K.; et al. Global patterns and climatic controls of forest structural complexity. *Nat. Commun.* **2021**, *12*, 519. [CrossRef]
42. Willim, K.; Stiers, M.; Annighöfer, P.; Ammer, C.; Ehbrecht, M.; Kabal, M.; Stillhard, J.; Seidel, D. Assessing understory complexity in beech-dominated forests (*Fagus sylvatica* L.) in Central Europe—From managed to primary forests. *Sensors* **2019**, *19*, 1684. [CrossRef] [PubMed]
43. Stolpe, N.; Undurraga, P. Long term climatic trends in Chile and effects on soil moisture and temperature regimes. *Chil. J. Agric. Res.* **2016**, *76*, 487–496. [CrossRef]
44. Bitterlich, W. Die Winkelzählprobe. *Forstwissenschaftliches Centralblatt* **1952**, *71*, 215–225. [CrossRef]
45. Kramer, H.; Akca, A. *Leitfaden zur Waldmesslehre*; 266 S; JD Sauerländer's Verlag: Göttingen, Germany, 2002.
46. Bannister, J.; Donoso, P. Forest typification to characterize the structure and composition of old-growth evergreen forests on Chiloe Island, North Patagonia (Chile). *Forests* **2013**, *4*, 1087–1105. [CrossRef]
47. Donoso, P.J.; Soto, D.P. Does site quality affect the additive basal area phenomenon? Results from Chilean old-growth temperate rainforests. *Can. J. For. Res.* **2016**, *46*, 1330–1336. [CrossRef]
48. Donoso, C. *Estructura y Dinámica de los Bosques del Cono sur de América*; Edición Universidad Mayor: Santiago, Chile, 2015; 406p.
49. Donoso, P.J.; Lusk, C.H. Differential effects of emergent Nothofagus dombeyi on growth and basal area of canopy species in an old-growth temperate rainforest. *J. Veg. Sci.* **2007**, *18*, 675–684. [CrossRef]
50. Veblen, T.T.; Schlegel, F.M.; BEscobar, R. Structure and dynamics of old-growth Nothofagus forests in the Valdivian Andes, Chile. *J. Ecol.* **1980**, *68*, 1–31. [CrossRef]
51. Fajardo, A.; González, M.E. Replacement patterns and species coexistence in an Andean Araucaria–Nothofagus forest. *J. Veg. Sci.* **2009**, *20*, 1176–1190. [CrossRef]
52. Miranda, A.; Hernández, H.J.; Bustamante, R.; Díaz, E.; González, L.A.; Altamirano, A. Regeneración natural y patrones de distribución espacial de la palma chilena Jubaea chilensis (Molina) Baillon en los bosques mediterráneos de Chile central. Gayana. *Botánica* **2016**, *73*, 54–63. [CrossRef]
53. Gutiérrez, J.R.; Arancio, G.; Jaksic, F.M. Variation in vegetation and seed bank in a Chilean semi-arid community affected by ENSO 1997. *J. Veg. Sci.* **2000**, *11*, 641–648. [CrossRef]
54. Fick, S.E.; Hijmans, R.J. Worldclim 2: New 1-km spatial resolution climate surfaces for global land areas. *Int. J. Climatol.* **2017**, *37*, 4302–4315. [CrossRef]
55. Oyarzún, C.E.; Godoy, R.; Staelens, J.; Donoso, P.; Verhoest, N.E. Seasonal and annual throughfall and stemflow in Andean temperate rainforests. *Hydrol. Process.* **2011**, *25*, 623–633. [CrossRef]
56. Luzio Leighton, W. *Suelos de Chile*; Impresos Maval: Santiago, Chile, 2010; 364p.
57. González, M.E.; Veblen, T.T.; Sibold, J.S. Fire history of Araucaria–Nothofagus forests in Villarrica National Park, Chile. *J. Biogeogr.* **2005**, *32*, 1187–1202. [CrossRef]
58. Pliscoff, P. Climatología. In *Parque Nacional La Campana: Origen de Una Reserva de la Biosfera en Chile Central*, 2nd ed.; Elórtegui, S., Moreira Muñoz, A., Eds.; Taller La Era: Viña del Mar, Chile, 2009; pp. 22–26.

59. Bannister, J.R.; Vidal, O.J.; Teneb, E.; Sandoval, V. Latitudinal patterns and regionalization of plant diversity along a 4270-km gradient in continental Chile. *Austral Ecol.* **2012**, *37*, 500–509. [CrossRef]
60. McGarigal, K.; Marks, B. *Fragstats: Spatial Pattern Analysis Program for Quantifying Landscape Structure. Vers. 2*; U.S. Department of Agriculture, Forest Service, Pacific Northwest Research Station: Corvallis, OR, USA, 1994; Volume 141, p. 7.
61. Zheng, G.; Moskal, L.M.; Kim, S.H. Retrieval of effective leaf area index in heterogeneous forests with terrestrial laser scanning. *IEEE Transit. Geosci. Remote Sens.* **2013**, *51*, 777–786. [CrossRef]
62. Ehbrecht, M.; Schall, P.; Ammer, C.; Fischer, M.; Seidel, D. Effects of structural heterogeneity on the diurnal temperature range in temperate forest ecosystems. *For. Ecol. Manag.* **2019**, *432*, 860–867. [CrossRef]
63. Wood, S.N. *Generalized Additive Models: An Introduction with R*, 2nd ed.; Chapman and Hall/CRC Texts in Statistical Science; CRC Press: Portland, OR, USA, 2017.
64. Otto, S.A.; Diekmann, R.; Flinkman, J.; Kornilovs, G.; Möllmann, C. Habitat heterogeneity determines climate impact on zooplankton community structure and dynamics. *PLoS ONE* **2014**, *9*, e90875. [CrossRef]
65. Ciannelli, L.; Chan, K.-S.; Bailey, K.M.; Stenseth, N.C. Nonadditive effects of the environment on the survival of a large marine fish population. *Ecology* **2004**, *85*, 3418–3427. [CrossRef]
66. Von Oertzen, T.; Brandmaier, A.M.; Tsang, S. Structural equation modeling with Ωnyx. *Struct. Equ. Model. Multidiscip. J.* **2015**, *22*, 148–161. [CrossRef]
67. Korhonen, L.; Korhonen, K.T.; Stenberg, P.; Maltamo, M.; Rautiainen, M. Local models for forest canopy cover with beta regression. *Silva Fenn.* **2007**, *41*, 671–685. [CrossRef]
68. Bolstad, P.V.; Elliott, K.J.; Miniat, C.F. Forests, shrubs, and terrain: Top-down and bottom-up controls on forest structure. *Ecosphere* **2018**, *9*, e02185. [CrossRef]
69. Chrimes, D.; Nilson, K. Overstorey density influence on the height of Picea abies regeneration in northern Sweden. *Forestry* **2005**, *78*, 433–442. [CrossRef]
70. Comeau, P.; Heineman, J.; Newsome, T. Evaluation of relationships between understory light and aspen basal area in the British Columbia central interior. *For. Ecol. Manag.* **2006**, *226*, 80–87. [CrossRef]
71. Rodríguez-Calcerrada, J.; Mutke, S.; Alonso, J.; Gil, L.; Pardos, J.A.; Aranda, I. Influence of overstory density on understory light, soil moisture, and survival of two underplanted oak species in a Mediterranean montane Scots pine forest. *For. Syst.* **2008**, *17*, 31–38. [CrossRef]
72. Donoso, P.J.; Ponce, D.B.; Pinto, J.B.; Triviño, I.L. Cambios en cobertura y regeneración arbórea en bosques siempreverdes en diferentes estados sucesionales en el sitio experimental de Llancahue, Cordillera de la Coa de Valdivia, Chile. *Gayana Bot.* **2018**, *75*, 657–662. [CrossRef]
73. Bannister, J.R.; Kremer, K.; Carrasco-Farías, N.; Galindo, N. Importance of structure for species richness and tree species regeneration niches in old-growth Patagonian swamp forests. *For. Ecol. Manag.* **2017**, *401*, 33–44. [CrossRef]
74. Enoki, T.; Abe, A. Saplings distribution in relation to topography and canopy openness in an evergreen broad-leaved forest. *Plant Ecol.* **2004**, *173*, 283–291. [CrossRef]
75. Machado, J.L.; Reich, P.B. Evaluation of several measures of canopy openness as predictors of photosynthetic photon flux density in deeply shaded conifer-dominated forest understory. *Can. J. For. Res.* **1999**, *29*, 1438–1444. [CrossRef]
76. McCarthy, B.C.; Robison, S.A. Canopy openness, understory light environments, and oak regeneration. In *Characteristics of Mixed Oak Forest Ecosystems in Southern Ohio Prior to the Reintroduction of Fire*; Sutherland, E.K., Hutchinson, T.F., Eds.; US Department of Agriculture, Forest Service, Northeastern Research Station: Newtown Square, PA, USA, 2003; Volume 299, pp. 57–66.
77. Majasalmi, T.; Rautiainen, M. The impact of tree canopy structure on understory variation in a boreal forest. *For. Ecol. Manag.* **2020**, *466*, 118100. [CrossRef]
78. Donoso, C. *Estructura, Variación y Dinámica de Bosques Templados de Chile y Argentina*; Ecología Forestal; Editorial Universitaria: Santiago, Chile, 1993; 369p.
79. Suarez, M.L.; Kitzberger, T. Differential effects of climate variability on forest dynamics along a precipitation gradient in northern Patagonia. *J. Ecol.* **2010**, *98*, 1023–1034. [CrossRef]
80. Soto, D.P.; Donoso, P.J.; Zamorano-Elgueta, C.; Rios, A.I.; Promis, A. Precipitation declines influence the understory patterns in Nothofagus pumilio old-growth forests in northwestern Patagonia. *For. Ecol. Manag.* **2021**, *491*, 119169. [CrossRef]
81. Asner, G.P.; Carlson, K.M.; Martin, R.E. Substrate age and precipitation effects on Hawaiian forest canopies from spaceborne imaging spectroscopy. *Remote Sens. Environ.* **2005**, *98*, 457–467. [CrossRef]
82. Holdridge, R. *Life Zone Ecology*; Tropical Science Center: San Jose, Costa Rica, 1967; 206p.
83. Whittaker, R.H. *Communities and Ecosystems*; Macmillan: Princeton, NJ, USA, 1970.
84. Robinson, T.M.; La Pierre, K.J.; Vadeboncoeur, M.A.; Byrne, K.M.; Thomey, M.L.; Colby, S.E. Seasonal, not annual precipitation drives community productivity across ecosystems. *Oikos* **2013**, *122*, 727–738. [CrossRef]
85. Tague, C.; Peng, H. The sensitivity of forest water use to the timing of precipitation and snowmelt recharge in the California Sierra: Implications for a warming climate. *J. Geophys. Res. Biogeosci.* **2013**, *118*, 875–887. [CrossRef]
86. Pan, Y.; Birdsey, R.A.; Phillips, O.L.; Jackson, R.B. The structure, distribution, and biomass of the world's forests. *Annu. Rev. Ecol. Evol. Syst.* **2013**, *44*, 593–622. [CrossRef]